Wind-Forced Variability of the Deep Eastern North Pacific: Observations of Seafloor Pressure and Abyssal Currents

P. P. Niiler,[1] J. Filloux,[1] W. T. Liu,[2] R. M. Samelson,[3] J. D. Paduan,[1] and C. A. Paulson[4]

Data from an array of bottom pressure gauges and a string of current meters in the vicinity of 47°N, 139°W, are used to examine the deep-ocean variability forced by ocean surface wind stress curl from August 1987 to June 1988. Bottom geostrophic currents are computed from the pressure gauge array, and these correspond well to the long-period directly measured currents at 3000 m. The supratidal-period bottom pressure variations are coherent at 95% confidence with the wind stress curl in period bands of 3–4 days and 15–60 days but removed in distances of 400 and 700 km to the northwest and the southeast, respectively. A linear, two-layer hydrodynamic model is used to examine the theoretical forcing produced by random-phased surface wind fields for the conditions of the eastern north Pacific and the 15- to 60-day-period observed response is reproduced credibly. To model 3- to 15-day variations, more realistic models are required.

1. Introduction

The first observations that time-dependent, deep-ocean currents are related to surface winds were derived from yearlong current meter records in a cluster of moorings north and east of Barbados. *Koblinsky and Niiler* [1982] showed that significant coherences existed between the 4- to 40-day-period east-west pulsations of the trade winds τ^x above Barbados and the north-south currents v at all depths in the ocean at 15°N, 54°W. The response amplitude of v to τ^x was depth- and period-dependent. It decreased by a factor of 3 from 150- to 4000-m depths and increased by a factor of 5 from 8- to 40-day periods. The interpretation of these data was that the deep-ocean forcing was produced by large horizontal scale wind stress curl (hereinafter referred to simply as "curl") due to westward propagating pulses in the trade winds with larger east-west than north-south scale. The amplitude of the deep wind-related currents was 1–3 cm/s. Thus deep-ocean forcing should be observable in many places where the mesoscale eddy energy is low.

Theoretically, wind-forced deep-ocean motions should depend upon wind stress curl. *Müller and Frankignoul* [1981], using a model of randomly forced linear motions in a stratified, infinite, flat-bottom, beta-plane ocean, computed local coherences and showed that motions across the planetary vorticity gradient should exhibit the strongest coherence with the local wind stress curl. *Niiler and Koblinsky* [1985], using current meter data, demonstrated that such a dynamical link does in fact exist locally at 42°N, 152°W, although at a shorter period than was predicted by Müller and Frankignoul. Both the amplitude and the phase of the currents that were forced across the planetary potential vorticity field (or f/H contours) on a 150-km horizontal scale were predicted from the local surface wind stress computed from a similar 150-km-scale wind field. The 4000-m oscilla-

tions in velocity at this site were shown to dynamically follow the steady state Sverdrup relationship, expressed as,

$$H^2 \mathbf{v} \, \nabla - (f/H) = \mathbf{z} \cdot \nabla - x(\tau/\rho), \qquad (1)$$

where H is the ocean depth, $\mathbf{v}$ is the horizontal velocity, f is the Coriolis parameter, τ is the surface wind stress, ρ is the density of seawater, and $\mathbf{z}$ is the unit vector in the vertical direction.

That deep-ocean motions that are perpendicular to the planetary vorticity gradient should show a wind-forced component has also been suggested by measurements of currents along the continental rise in the northeastern Atlantic. *Dickson et al.* [1982] analyzed current meter data from six sites in the eastern North Atlantic between 41° and 59°N. Record lengths ranged from 5 to 25 months, and depths ranged from 200 to 4700 m. They showed that the eddy kinetic energy of motions with periodicities between 3 and 80 days along topographic contours increased in winter by a factor of 5. Because mesoscale wind forcing at these latitudes has a strong seasonal cycle, they suggested that the increased current variability in winter was caused by the concurrent increase of atmospheric variability. In the analysis of 3 years of deep-ocean currents from 42°N, 152°W, *Koblinsky et al.* [1989] showed that in the direction of the planetary vorticity gradient, variable currents of annual and interannual time scale followed the variability of the mesoscale curl at that location. Thus the seasonally forced local response was established. However, in a survey of 31 sites in the Pacific for which an excess of 1 year of current meter data exists, they found only three locations where a local relationship of wind curl and currents could be established. *Cummins* [1991] used a barotropic, variable-depth model of the northeast Pacific and forced it with random, white-spectrum wind stress curl. He found that local planetary vorticity balance was established only for large (4° × 4°) area averages of the velocity and at periods larger than 40 days. In models, bottom topography produces many small-scale, incoherent waves. *Cummins*'s [1991] calculations with a three-layer baroclinic model, but now forced with European Center for Medium-Range Weather Forecasts (ECMWF) winds, also demonstrated that the wintertime increase of kinetic energy at the lowest level is not necessarily a consequence of local planetary vorticity tendency but is most likely a consequence of increased wintertime, barotropic wave activity.

[1]Scripps Institution of Oceanography, La Jolla, California.

[2]Jet Propulsion Laboratory, Pasadena, California.

[3]Woods Hole Oceanographic Institution, Woods Hole, Massachusetts.

[4]College of Oceanic and Atmospheric Sciences, Oregon State University, Corvallis.

The theoretical framework of how both components of motion are forced by curl and how, in a more general sense, coherence analyses can be used to examine deep-ocean forcing by curl was extended in an important way by *Brink* [1989]. He noted that since the wind response should be quasi-geostrophic, Rossby waves (or topographic Rossby waves) that are excited by the curl should transport information, or coherence, along the direction that wave groups travel. Both eastward and westward propagation of information in the deep ocean is possible. His inclusion of wave dynamics in the search for deep-ocean response was motivated by the work of *Allen and Denbo* [1984], who observed in the analysis of wind-forced continental shelf motions, where the continental shelf waveguide is very strongly oriented alongshore, that motions along f/H contours are most coherent with wind forcing removed some distance from the measurement site, opposite the direction of wave group propagation. *Brink* [1989] showed theoretically that the strongest coherence in a randomly forced ocean should be nonlocal because of Rossby wave propagation and, indeed, discovered that deep currents at 28°N, 70°W were more strongly coherent with curl to the east of this site than with the local curl, although predicted and observed energy levels differed by 2 orders of magnitude. *Samelson* [1990] compared a similar model with observations from current meters at 32°N, 24°W and found reasonable agreement in deep energy levels and in coherence patterns for 3.7- to 8.0-day-period motions, especially when a reflecting midocean ridge was included along with the absorbing eastern and western boundaries. These results suggested the possible existence of wind-forced, standing planetary waves at 3.7- to 8.0-day periods in the eastern North Atlantic basin, although only one reflection, rather than the two needed for a standing wave, was allowed in the model.

The theories of Brink and Samelson predict that typically the strongest coherence should be between bottom pressure and curl. *Luther et al.* [1990] demonstrated, with a yearlong bottom pressure and barotropic velocity determined from electric field measurements at 41°N, 169°W, that significant nonlocal coherences can be found between the bottom pressure, "electromagnetic" barotropic velocity, and curl in the period band between 2 and 25 days. The observed coherence was considerably larger than that predicted. The large-period coherence was strongest with the forcing to the southeast of the bottom record location and was 180° out of phase, while the small-period response exhibited a coherence maximum directly over the pressure sensor, with phase decreasing to the west. In our paper we find several qualitative aspects of agreement of Samelson's theory with both our observations and those of *Luther et al.* [1990].

In summary, we now know that wind-forced deep-ocean motions are observable and that strong, wintertime wind stress variability produces the strongest deep currents. Theory suggests that in the open ocean, the field most coherent with the surface forcing should be bottom pressure. The motions across f/H contour should also have an observable coherent response to the curl at distances removed from the observation site which depend upon the period of the forcing. For small periods (few days or strictly $\omega < f$), the highest coherences are expected to be local, while for large periods (but smaller than the values for which the Sverdrup balance is established), the remote forcing will play an increasingly important role. Theoretically and observation-

ally, it is found that motions along f/H contours on continental shelves and margins, where trapped waves are possible, exhibit significant remote coherences with wind forcing. In the open ocean, barotropic components should be present at all latitudes and observations, and theory shows that both velocity components are coherent. Both eastward and westward propagation of information from a forcing area should be expected. In mid to high latitudes, the motions should not exhibit significant baroclinic forced components for 2- to 40-day periodicities.

In August 1987, as part of the Ocean Storms experiment, we placed a coherent array of seven bottom pressure gauges and a string of deep current meters in the vicinity of 47°N, 139°W, to observe the deep-ocean response to surface forcing in a detailed fashion, which had not been possible before. The array of instruments was recovered in June 1988. This is a report of an observational and theoretical synthesis of the relationship between wind forcing and deep response in the eastern North Pacific. In section 2 the array of instruments and the data series are discussed, in section 3 the relationships between wind stress curl and deep-ocean variability are analyzed, in section 4 a theoretical model is compared with the observations, and the conclusions are presented in section 5.

2. THE DATA

The array of sensors was deployed from R/V *Melville* in the period August 22–27, 1987, and recovered during the period June 18–25, 1988. Figure 1a shows the array location and configuration superimposed on a 2° spatial average field of f/H contours. Figure 1b shows the detailed locations, within the topographic features, of the array of bottom pressure sensors and the current meter mooring from which good data were obtained. A discussion of the pressure sensor principles, performance, drift correction procedures, and data reduction is given by *Filloux* [1980, 1983]. The current meters were deployed on a taut-wire, subsurface mooring with an Aanderaa acoustic current meter at 3000 m. The detailed instrument performance, methods of data reduction, and raw statistics are given by *Levine et al.* [1990]. Here we use bottom pressure records which were low passed with a 38-hour Doodson filter to remove tidal signals and the current meter record from 3000-m depth, which was averaged daily. All records were decimated to 0.2-day intervals.

The wind stress data were obtained from the ECMWF 6-hourly surface analysis on a 2.5° × 2.5° stereographic grid (a separate analysis with the National Meteorological Center data produced no significant differences). The surface winds and other boundary layer parameters were used to produce a wind stress according to the scheme of *Liu et al.* [1979] under neutral conditions. Curls were computed on a central finite-difference scheme.

There was such a high degree of similarity between the six recovered pressure records (Figure 2) that we restrict our analysis and interpretation to data from the central site (P7). However, there are also small but significant differences in the amplitudes of the pressure signals which we used to compute the pressure gradients. The 300-day record of utility to us contains the infratidal pressure variations with periodicities of up to about 50 days. At longer periods the signals become severely contaminated by the inelastic re-
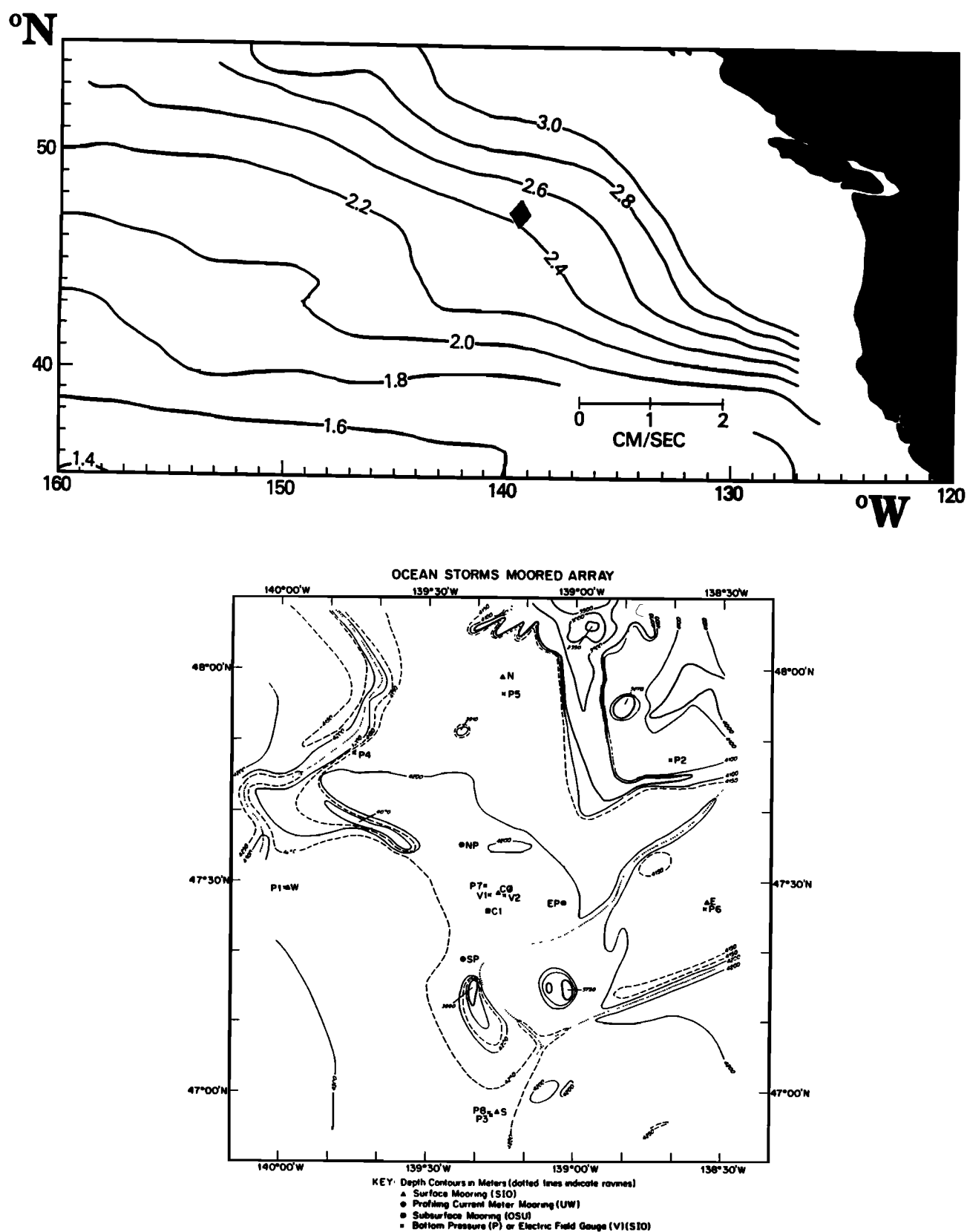
Fig. 1.   Locations (top) of the instrumented array on 2° spatial average f/H contours (in units of 10^{-12} cm^{-1} s^{-1}) and (bottom) of bottom pressure gauge (squares) and deep current meter (square labeled C1) in Ocean Storms.
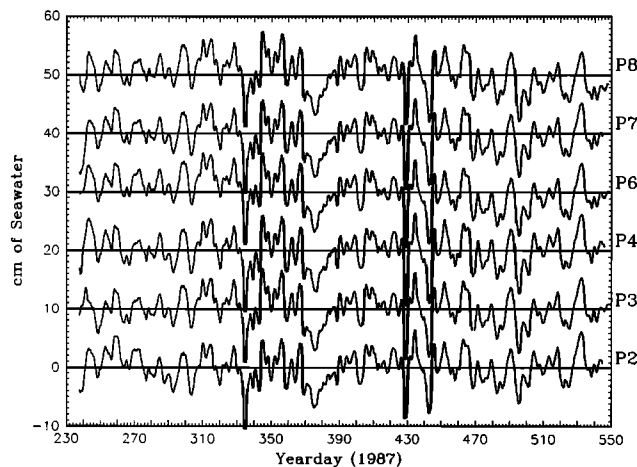
Fig. 2. The long-period records of bottom pressure from Ocean Storms, which have been passed through a 38-hour-cutoff Doodson filter.

sponse, or creep, of the sensor under the stress of a 4200-m water pressure head. This longer-period limitation is discussed by *Filloux et al.* [1991]. It is also illustrated in Figure 3, which displays the pressure difference between the two closest sites (P3 and P8), and discussed further in the appendix, which describes the insights into pressure sensor behavior gained from the present study.

To provide a realistic, independent, quantitative assessment of the creep-corrected data and their significance, we computed the horizontal pressure gradient within the array by fitting, in a least squares sense, a quadratic function of longitude and latitude to the pressure signals and evaluated it at the location of the current meter mooring. Since the currents with periods longer than 10 times 17.4 hours (the inertial period) should be within 10% of geostrophic equilibrium, a comparison of the geostrophic currents computed from this pressure gradient with the measured currents should further define the useful frequency range of the pressure records. Figure 4 shows the comparison of the directly measured current components with the geostrophi-
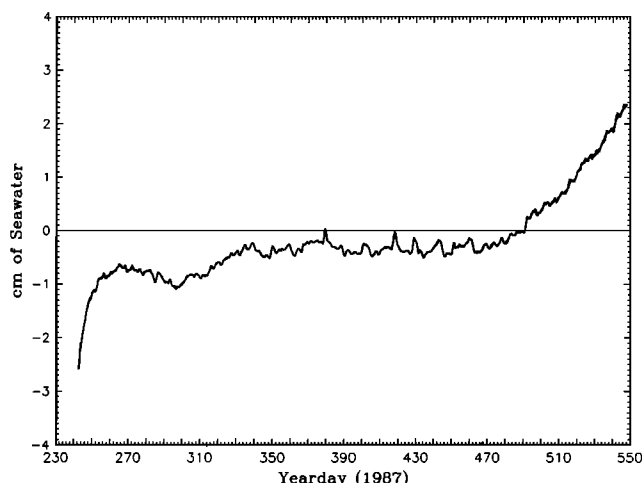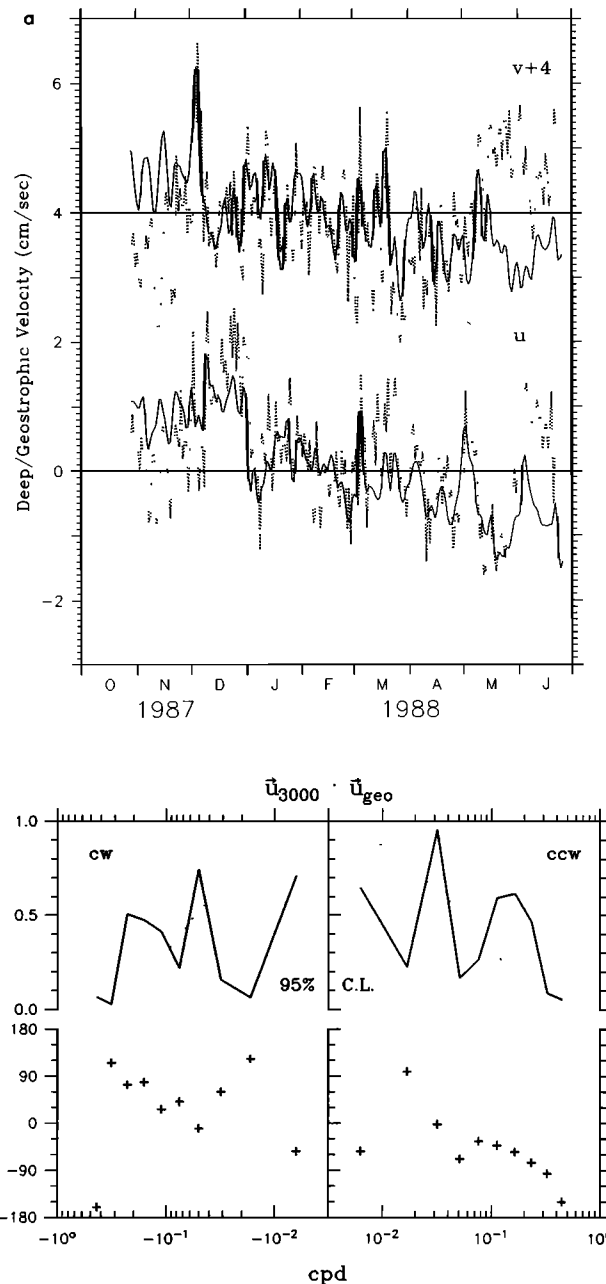

Fig. 4. (*a*) Directly measured currents at 3000-m depth (dotted line) and geostrophically computed currents from the bottom pressure array (solid line); (*b*) rotary coherence and phase of the measured and computed currents. Positive phase means computed currents lead the measured currents. The dotted line is the 95% confidence level.

Fig. 3. Pressure differences between P3 and P8, which were separated by 0.5 km.

cally determined components from the pressure array. The trends in pressure difference (Figure 4*a*) which are not reproduced in the corresponding directly measured currents further demonstrate that these pressure data must be used with appropriate care, particularly at longer periods. It is expected, however, that the coherence between currents measured at a single point at 3000-m depth and those averaged over the separation distances between pressure sensors at 4200-m depth would be less than unity. We do not have information on the spatial scale of currents in this area, so we cannot estimate what the true coherence should be

TABLE 1. Parameters of the Two-Layer, Stochastically Forced Model

Description	Definition and/or Value Used
Layer depths	$D_1 = 700$ m
	$D_2 = 3500$ m
Reduced gravity	$g\Delta\rho/\rho = 1$ cm s^{-2}
Coriolis parameters	$f = 1.1 \times 10^{-4}$ s^{-1}
	$\beta = 1.6 \times 10^{-13}$ cm^{-1} s^{-1}
Effective β magnitude	$\beta = H|\nabla f/H| = 3.2 \times 10^{-13}$ cm^{-1} s^{-1}
Effective β direction	$18°$ T
Fraction parameter	$R = (180$ days$)^{-1}$
Eastern boundary	$X = 1250$ km from site in lower layer
Autocorrelation for curl	$T(x, y) = \exp(-\sigma|x| - s|y|)^*$

*For 3-day period, $\bar\sigma^{-1} = 750$ km and $\bar{s}^{-1} = 250$ km, and for 25 day period, $\bar\sigma^{-1} = 1200$ km and $\bar{s}^{-1} = 500$ km.

compared with that computed from the pressure array as shown in Figure 1. Because a significant coherence was computed between these two time series in the period band 3 to 40 days (Figure 4b), we felt it was legitimate to use the pressure data in this period interval to relate bottom pressure to surface forcing. Note that in the 3-day-period motions, the current meter record leads the bottom pressure record, implying a vertical-phase propagation in the 3-day-period signal. This is the first time we are aware of that a pressure gradient has been measured with sufficient precision and proper spatial scale to be used to derive an absolute two-dimensional current from the geostrophic momentum balance.

3. THE OBSERVED DEEP RESPONSE TO SURFACE FORCING

As we have pointed out, the atmospheric forcing of ocean bottom currents and pressure in time periods of a few days to a few months is caused primarily by the curl (see works cited in the introduction). Measurable forcing by atmospheric surface pressure distributions is not expected, because the surface pressure distributions over our site have horizontal scales of less than 1250 km in periods of less than 25 days (Table 1), and these are smaller than the barotropic radius of deformation. If H is a constant water depth and the atmospheric pressure has a horizontal scale L, then isostasy will occur if $(L/R)^2 \ll 1$, where $R^2 = (gH)/f^2$ is the square of the barotropic deformation radius of 2000 km. An isostatic, or inverse barometer, response of the sea level is expected. We computed the correlations of the bottom pressure with the local atmospheric pressure, and they were not significant in any period band between 3 and 50 days, which is consistent with local isostasy (this can also be seen from the phase and coherence structures in Plate 4). Of course, significant correlations are found between bottom pressure and atmospheric pressure (or winds) removed in space or lagged in time, but those are produced by the features in the sea level pressure (and winds) which produce a curl of the wind stress. So, we go directly to the analysis of bottom response in terms of the curl. Some of the most dramatic relationships of the associated atmospheric pressure distributions to the bottom pressure and velocities at 3000 m are also demonstrated.

We computed the spatial distribution of coherence and phase between bottom pressure and curl as a function of period over the area 35°–60°N, 120°–160°W. The record

length of instrument P7 (Figure 2) is 300 days; averaged raw estimates of the cospectra and quadspectra were used to produce band-averaged coherence and phase estimates as a function of period. Coherence estimates above 95% confidence limits were found in the 3- to 4-day-period band and the 15- to 60-day-period band. The 3- to 4-day-period variability of the bottom pressure is most coherent with the curl 400 km to the northwest; the phase increases across this area from east to west (Plate 1). The 15- to 60-day-period bottom pressure was most coherent with curl 400–700 km to the southeast, which follows remarkably the direction from which energy of the large-scale topographic Rossby waves would propagate to the bottom pressure site along (f/H) contours (Figure 1); the phase is nearly constant at 180° (Plate 1). These results are quantitatively similar, both in amplitude of the coherence and in phase, to those of Luther et al. [1990], who used similar-length bottom pressure records from 1986–1987 at 40.7°N, 169.3°W. Thus the northward location of the small-period coherence and the southeastward location of the large-period coherence maxima between bottom pressure and curl are firmly established at the two sites for which yearlong bottom pressure measurements exist.

The 3000-m-depth northward velocity has significant coherence with the curl located 200 km to the north of the mooring in the 3- to 4-day band and 600 km to the northeast in the 9- to 33-day band (Plate 2). We also computed the geostrophically derived northward current coherence with the curl, and no essential differences were found. The coherence between eastward current and the curl (Plate 3) was lower than with bottom pressure and northward velocity; at a few locations, 95% significant coherences appeared at period bands of 4.5 and 15–60 days, which appear to be at longer periods than the significant coherences observed for the northward component (Plate 2). Since bottom pressure variations are caused by the deep currents, it is not surprising that the bottom pressure coherence spans the bands of the combined velocity coherences.

Because surface winds are proportional to geostrophic winds, the curl is a twice-differentiated function of the atmospheric surface pressure, being nearly proportional to Laplacian of pressure. In the atmospheric systems that travel through our observational site, Laplacian pressure is proportional to pressure itself (with a negative sign) because the time-dependent pressure systems are "bowl-shaped." Thus the coherence pattern expected between the curl and surface pressure is similar to that observed between the curl and bottom pressure (with a 180° phase shift). This relationship is not, however, a dynamical one but rather is caused purely by the nature of the self-coherence of the atmospheric variables (for similar reasons, we expect to have coherence of the deep measurements with the surface winds). Differentiation introduces noise. Therefore the coherence patterns obtained using atmospheric pressure are expected to be at a higher significance level than those obtained using the curl. This is dramatically demonstrated in the coherence patterns of bottom pressure and velocity with atmospheric pressure (Plates 4–6). The atmospheric pressure coherences mirror the curl coherences but at a larger level of significance. Note that over the bottom pressure array, there is no correlation (coherence at 0° or 180° phase) of bottom pressure and atmospheric pressure.

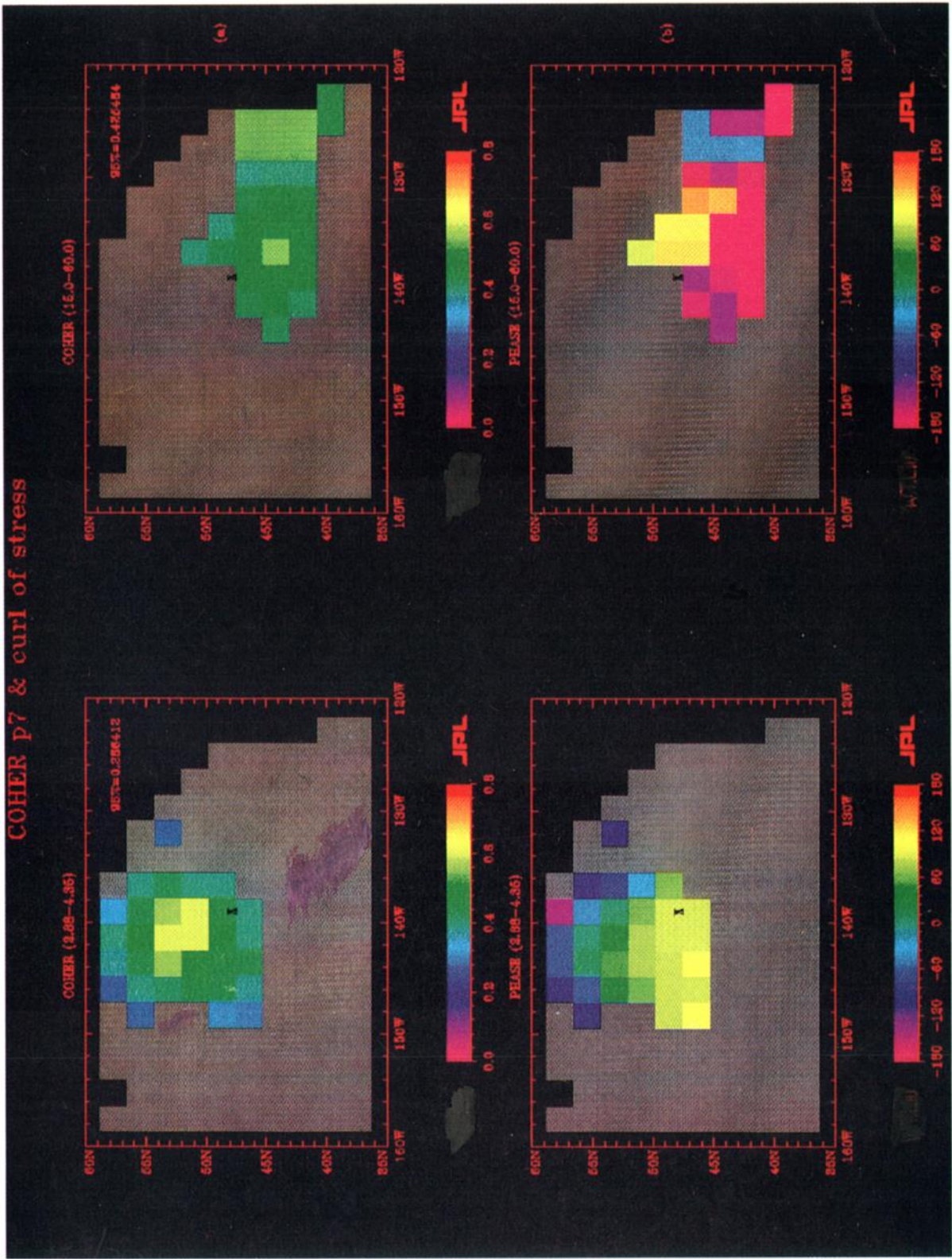A computation of the steric level determined from temper-

Plate 1. Spatial distribution of (*a*) coherence and (*b*) phase between curl and bottom pressure in (left) 3- to 4-day band and (right) 15- to 60-day band. The location of the pressure gauge is marked by a cross. The 95% confidence estimate for coherence is marked in Plate 1*a*.
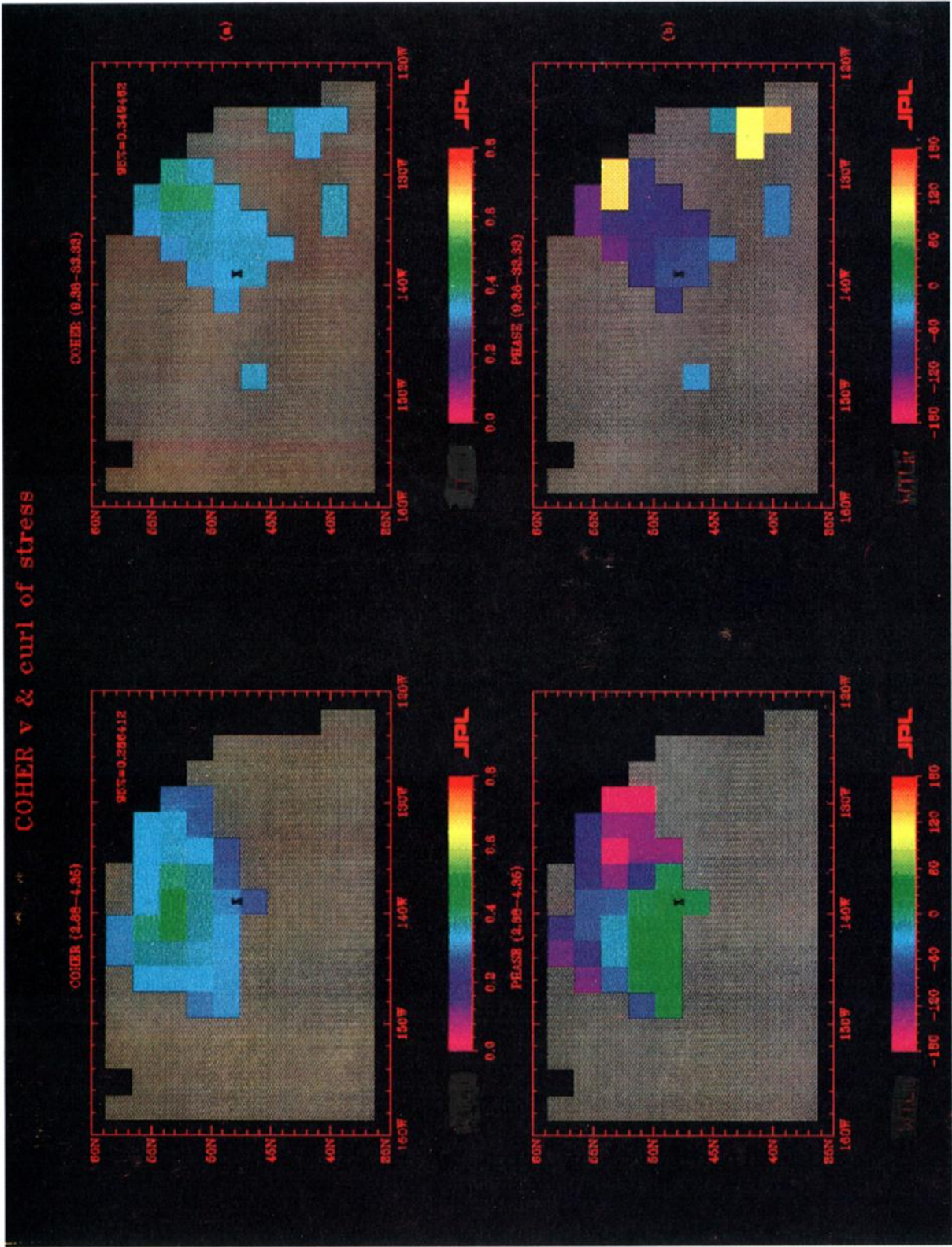
Plate 2. Spatial distribution of (a) coherence and (b) phase between curl and 3000-m directly measured northward current in (left) 3- to 4-day band and (right) 9- to 33-day band. The location of the current meter is marked by a cross. The 95% confidence estimate for coherence is marked in Plate 2a.
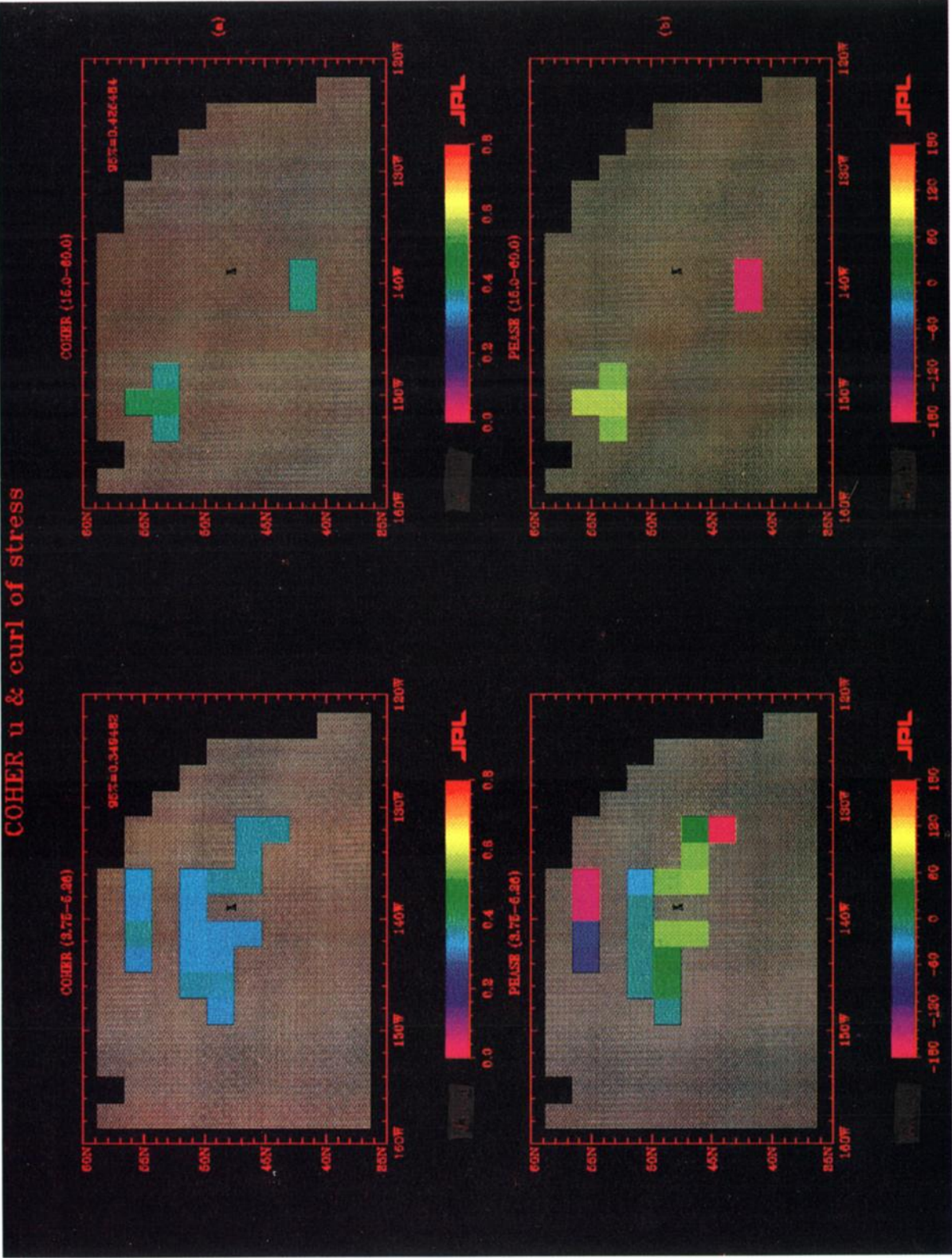
Plate 3. Spatial distribution of (*a*) coherence and (*b*) phase between curl and 3000-m directly measured eastward current in (left) 4- to 6-day band and (right) 15- to 60-day band. The location of the current meter is marked with a cross. The 95% confidence estimate for coherence is marked in Plate 3*a*.
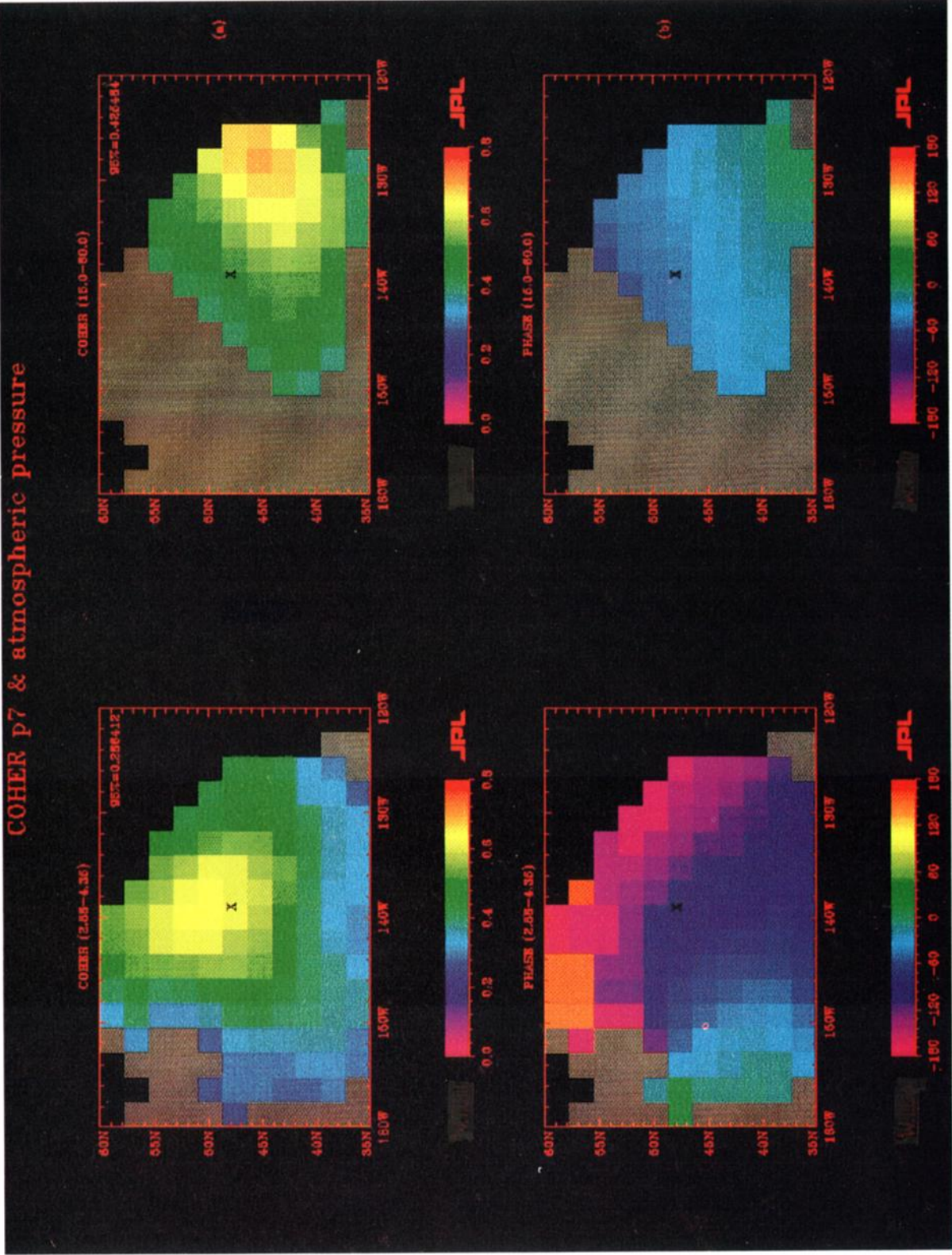
Plate 4. Spatial distribution of (*a*) coherence and (*b*) phase between atmospheric pressure and bottom pressure in (left) 3- to 4-day band and (right) 15- to 60-day band. The location of the pressure gauge is marked with a cross. The 95% confidence estimate for coherence is marked in Plate 4*a*.
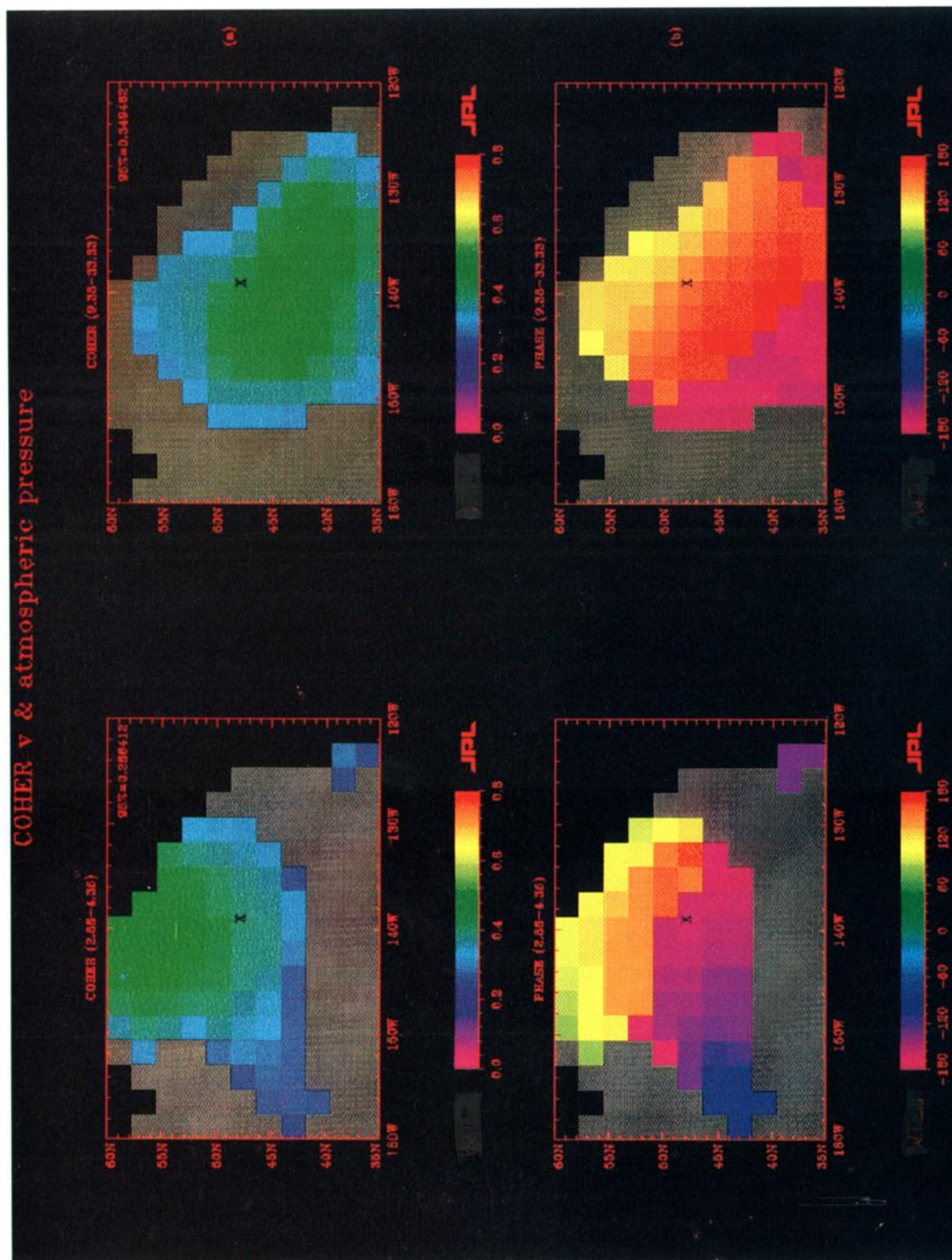
Plate 5. Spatial distribution of (*a*) coherence and (*b*) phase between atmospheric pressure and 3000-m directly measured northward current in (left) 3- to 4-day band and (right) 9- to 33-day band. The location of the pressure sensor is marked with a cross. The 95% confidence estimate for coherence is marked in Plate 5*a*.
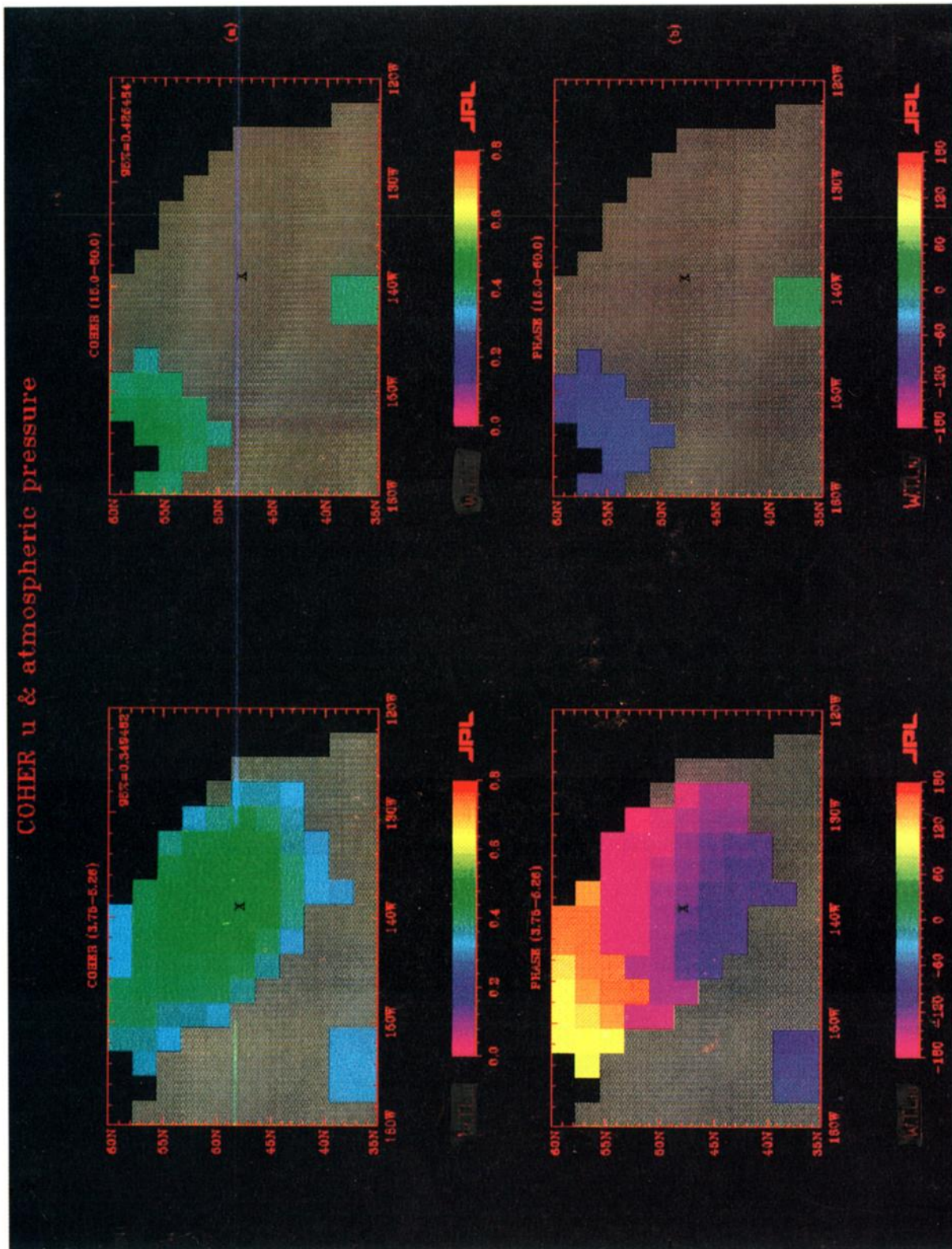
Plate 6. Spatial distribution of (*a*) coherence and (*b*) phase between atmospheric pressure and directly measured eastward current in (left) 4- to 6-day band and (right) 15- to 60-day band. The location of the current meter is marked with a cross. The 95% confidence estimate for coherence is marked in Plate 6*a*.

ature and salinity observations in the upper 200 m and temperature and water mass observations from 200–3000 m revealed no significant amplitude of wind coherent steric level changes in the periodicities considered here (but see *Tabata et al.* [1986] for steric level coherence with curl in interannual periods). Thus the sea level locally is consistent with the inverse barometer behavior. By virtue of their mutual coherence to sea level pressure, we are able to better separate the patterns of bottom pressure that are associated with the northward (3- to 4- and 9- to 33-day) and the eastward (4- to 5- and 15- to 60-day) components of the motion in the analysis of atmospheric pressure. We make this latter computation both to demonstrate the robustness of the observed forcing of the deep ocean by atmospheric variability and to provide a more comprehensive forum for ocean model and observation intercomparisons.

4. COMPARISONS WITH A STOCHASTICALLY FORCED MODEL

It is of considerable interest to ascertain whether simple models of ocean circulation can reproduce the more robust results of the observations described in this paper. One simple model is that of *Samelson* [1989], in which the response of a two-layer quasi-geostrophic ocean to a statistically homogeneous stochastic curl may be obtained in an analytically closed form, and the coherences can be rapidly evaluated numerically. This model is an extension of those initiated by *Müller and Frankignoul* [1981] and is similar to that of *Brink* [1989] but allows the introduction of a reflecting meridional barrier and can also include a gentle, uniform bottom slope. The space and time scales of the curl are not related, so a separable function of the frequency and wavenumber spectrum is assumed. Its chief virtue is that a large number of parameter studies can be done with great efficiency. We are aware that more realistic modeling efforts, with the observed winds and more realistic bottom variations and coastlines, are under way. We present the simplest model results here, because not only is it a first logical step to any theoretical interpretation, but also we were curious to learn which, if any, of the observed features of the responses could be replicated with the simplest ideas.

To use this model, estimates of the horizontal coherence scales of the curl as a function of period are required as input to the model. We computed the spatial distributions for the autocorrelation function of the curl for the period bands listed in Table 1. We estimated the horizontal coherence scales from an exponential function representation of these observations. Other parameters used in the model are also listed in Table 1.

As has been discussed by *Samelson* [1990], this model reproduces observed deep energy levels and several features of the spatial patterns of observed coherence between curl and deep currents in the eastern North Atlantic for 3.7- to 8.0-day-period motions. For our calculations, with the parameters appropriate to the eastern North Pacific, the robust model results were as follows.

1. The locations of the coherence maxima for a 3-day period were very near the observation site for bottom pressure and northward velocity and to the north of the observing site for the eastward velocity. The phase decreased to the west. The computed coherence maxima were 0.2–0.3 (Figure 5).

2. The locations of the coherence maxima for a 25-day period were to the southeast, along the lines of constant f/H, of the observing site for pressure and to the south of the
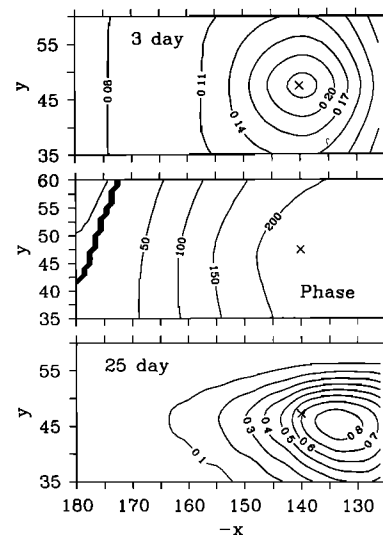

Fig. 5. Model-computed spatial distribution of (top) coherence and (middle) phase between curl, bottom pressure, and bottom currents at a period of 3 days, and (bottom) coherence between curl and bottom pressure at a period of 25 days (the phase is uniform at 180°). The model parameters are listed in Table 1. The x and y axes are in units of degrees west and degrees north, respectively.

observing site for northward velocity. The phase was uniform at 180°. The computed coherence maxima were 0.8–0.9 (Figure 6).

3. Removing the reflecting barrier at the eastern boundary reduced the coherence. *Samelson and Shrayer* [1991] have have modified the model to allow a meridionally varying curl amplitude (at the expense of removing the meridional boundaries and barrier), and their results indicate that the coherence maxima shift to the north when the curl amplitude increases to the north, as it does in the eastern North Pacific [*Evenson and Veronis*, 1975].

The major observed features which agree with the model computations are the general locations of the small- and large-period maxima of the coherences and, surprisingly, also the phases (recall the difference of the phase of the small-period currents measured at 3000 m and those determined from the bottom pressure array at 4200-m depth). The phases of randomly forced motions and those forced by the real curl patterns are expected to be different because of the traveling wave trains in the real atmosphere. An inclusion of a northward increasing curl could move the site of the computed coherence maxima northward and closer to the observed location (not done here because of the added complexity, which seemed not to be warranted). The major discrepancies are the very low levels of theoretical coherences at 3–5 days compared with the observations, though this may in part be corrected by increasing the bottom friction as a function of frequency. The observed low coherences with the eastward component of flow are not reproduced in the model. The observations suggest that either a strongly phase-locked and resonant basin mode of motion must be excited in the ocean (for Pacific Ocean basin modes, see *Miller* [1989]), or, as *Luther et al.* [1990] have pointed out, the 2- to 4-day-period curl is very ineffective at generating topographic Rossby waves because it tends to travel to the east. This latter effect is not included in the simple
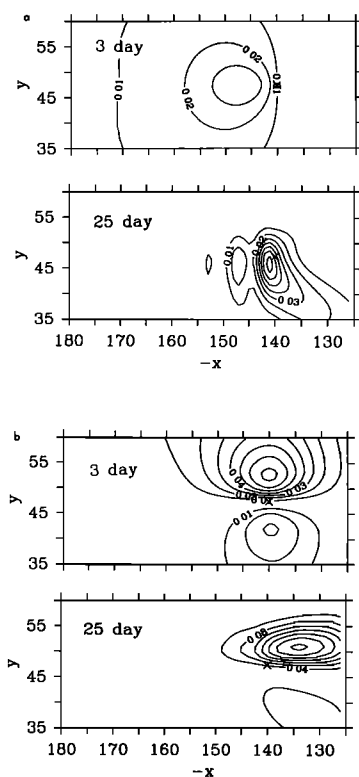
Fig. 6. Model-computed spatial distribution of squared coherence between curl and bottom currents at periods of 3 and 25 days for (a) northward component and (b) eastward component. The phase of both 3- and 25-day-period bands for v is similar to that of the bottom pressure (Figure 5). The model parameters are listed in Table 1. The x and y axes are in units of degrees west and degrees north, respectively.

models we used of the wavenumber and frequency structure of the curl.

5. Discussion

The understanding of the response of the deep ocean to surface wind forcing in periods of 2–60 days has dramatically improved in the last few years owing to the deployment of arrays of deep pressure sensors and velocity sensors, from which robust deep responses can be estimated, and to the use of simple models, from which nonlocal forcing can be calculated with relative ease. Our measurements of bottom pressure and near-bottom currents demonstrate that wind curl forces deep-ocean motions, and the associated deep pressure signals caused by these motions reveal the clearest, most coherent patterns: (1) 2- to 5-day-period bottom pressure variations are coherent with curl to the north of the observing site; (2) 15- to 60-day-period bottom pressure variations are coherent with curl to the south and east of the observing site; (3) the northward component of current is more coherent than the eastward component, and the former exhibits stronger relative coherences at shorter periods than the latter; and (4) the phase of the coherence is such that there is no local correlation between ocean bottom pressure and atmospheric pressure, a picture consistent with the expected theoretical isostasy of sea level fluctuations whose scale is less than 2000 km.

Our data also corroborate the evidence presented by Luther et al. [1990] that 15- to 60-day-period motions tend to

retain the coherence of the curl for a distance from the location where they were generated by simple constructive reinforcement of waves generated from that source. This striking similarity between these two sets of measurements over several period bands is an indication that at both sites there were similar wind-forced motions (but also note that Luther et al. [1990] did not find the 7- to 15-day-period coherence gap we found). Such a robust observation, because it was taken at different latitudes over different detailed bottom topographies and in different years, implies that several of its features should also be apparent in very simple models of wind-forced variability in the eastern North Pacific. The observed coherence with bottom pressure in the 15- to 60-day-period band is very similar indeed in both location and phase to that which is computed from the simplest stochastically forced model.

The 2- to 5-day-period oscillations were not as well modeled in the northeastern Pacific. This might be due to the fact that the stochastic models of the wind are not a good representation of the real curl in this period band, or it might be due to the latitudinal variations of the curl, which we did not model here in detail. The theoretical coherence estimate due to random forcing would be an underestimate of the expected, more realistic case in which the small-period winds propagate to the east and do not generate Rossby waves, which reduce the coherences. The random forced curls have equal components propagating to the east and the west. Also, a theoretical explanation as to why the 5- to 15-day-period variabilities near the bottom are not expected to be coherent with the surface forcing is missing. Our theory in simple basins would have the coherences in this band be simply halfway between those of the 2- to 5- and 15- to 60-day bands. Neither spectra of the curl nor bottom pressure shows a lack of energy at 5- to 15-day periodicities. The absence of a 7- to 15-day coherence at our location is a strong indication that in this period band, topographic Rossby waves from distant locations arrive at the site and interfere with the more local forcing. The qualitative reason is perhaps found in the computations by Luther et al. [1990] which show that in this period band, atmospheric disturbances over the northeastern Pacific travel increasingly to the northeast, a feature which is not modeled in the wavenumber and frequency spectrum used in our theoretical calculation. Finally, these simple models do not represent the smaller subbasins in topography which can exhibit semiresonances at this incoherent period band.

The overall result of modeling bottom pressure with stochastic models appears more realistic than modeling currents, and this is to be expected, because currents are more sensitive to the details of local bottom variations than is bottom pressure. The least well modeled feature, as well as the least coherent feature, is the eastward component (or the motion along the f/H contours). This is to be contrasted with the result from the continental shelf, where the best observed coherency and best modeled current are along the f/H contours. The principal differences between deep ocean and the shelf are that discrete, resonant modes (the shelf waves) can occur on the shelf and the local stratification is crucial to their structure, while in the deep ocean the response is barotropic to a very high degree and resonances are very difficult to excite.

As we have seen from Chave et al. [1991], the frequency and wavenumber spectra of wind stress curl computed over

a few years of time series are not stationary. This calls into question the utility of comparing statistically stationary models of wind forcing with several years of in situ ocean observations. Perhaps now is a propitious time to do more model computations which are forced with observed (assimilated) winds and which have realistic topographies, orographies, and stratifications [*Willebrand et al.*, 1980]. An excellent data set and an analysis framework now exists for interpreting and testing the verity of basin-wide computations of the time-dependent, wind-forced motions in the deep ocean.

APPENDIX: CORRECTIONS FOR PLASTIC FLOW OF PRESSURE SENSORS

From our drift-modeling exercise, we have learned that the selected semideterministic approach to plastic flow rejection did not use all information available and, in particular, that it did not perform as well as it ultimately could in the presence of a signal other than plastic deformation. This conclusion is evident from the discrepancy illustrated in Figure 3 between the drift-corrected records from two identical instruments that were closely spaced at the same water depth. The general shape of the error curve is that of a steep quadratic initial slope followed by a long period of small offset and ending in a sustained, nearly linear trend. The plastic flow expression is [*Filloux*, 1980]

$$A + B(T + C)^D$$

The results in Figure 3 suggest that an optimum D was not used. Choosing a D for either sensor in less than an optimum way would produce precisely the shape of the difference (or error) curve that we see in Figure 3. The difficulty of better determining the D parameters results from that portion of the deformation which is nonplastic in nature, which in turn produces an apparent coupling between parameters D and B. This coupling is manifested as a range of D (and B) values over which the misfit does not change rapidly.

On the basis of our experiences in this study, we recommend that for an array of pressure sensors, the final step in the selection of creep parameters should be a joint optimization that minimizes overall misfit of the ensemble of differences between all record pairs. This step should be combined with improved transducer construction methods now available that are capable of reducing stress and therefore plastic strain more rapidly (see discussion by *Filloux et al.* [1991]). Together, these improvements will provide the best possible rejection of creep-induced drift from actual seafloor pressure observations using relatively inexpensive instruments.

REFERENCES

Allen, J. S., and D. W. Denbo, Statistical characteristics of the large-scale response of coastal sea level to atmospheric forcing, *J. Phys. Oceanogr.*, *14*, 1079–1094, 1984.

Brink, K. H., Evidence for wind-driven current fluctuations in the western North Atlantic, *J. Geophys. Res.*, *94*(C2), 2029–2044, 1989.

Chave, A. D., D. S. Luther, and J. H. Filloux, Variability of the wind stress curl over the North Pacific: Implications for the

oceanic response measurements, *J. Geophys. Res.*, *96*(C10), 18,361–18,396, 1991.

Cummins, P. F., The barotropic response of the subpolar North Pacific to stochastic wind forcing, *J. Geophys. Res.*, *96*(C5), 8869–8880, 1991.

Dickson, R. R., W. J. Gould, P. A. Gurbutt, and P. P. Kilworth, A seasonal signal in the ocean currents to abyssal depths, *Nature*, *295*, 193–198, 1982.

Evenson, A. J., and G. Veronis, Continuous representation of wind stress and wind stress curl over the world ocean, *J. Mar. Res.*, *33*, suppl., 131–144, 1975.

Filloux, J. H., Pressure fluctuations on the open ocean floor over a broad frequency range: New program and early results, *J. Phys. Oceanogr.*, *10*, 1959–1971, 1980.

Filloux, J. H., Pressure fluctuations on the open ocean floor off the Gulf of California: Tides, earthquakes, tsunamis, *J. Phys. Oceanogr.*, *13*, 143–171, 1983.

Filloux, J. H., D. S. Luther, and A. D. Chave, Update on seafloor pressure and electric field observations from the north-central and northeastern Pacific: Tides, infratidal fluctuations and barotropic flow, in *Proceedings of First International Tidal Hydrodynamic Conference*, edited by B. Parker, John Wiley, New York, 1991.

Koblinsky, C. J., and P. P. Niiler, The relationship between deep ocean currents and winds east of Barbados, *J. Phys. Oceanogr.*, *12*, 144–153, 1982.

Koblinsky, C. J., P. P. Niiler, and W. J. Schmitz, Jr., Observations of wind-forced deep ocean currents in the north Pacific, *J. Geophys. Res.*, *94*(C8), 10,773–10,790, 1989.

Levine, M. D., C. A. Paulson, S. R. Gard, J. Simpkins, and V. Vervakis, Observations from the C1 mooring during OCEAN STORMS in the NE Pacific Ocean, August 1987–June 1988, *Ref. 90-3, Data Rep. 151*, Oreg. State Univ., Corvallis, 1990.

Liu, T., K. B. Katsaros, and J. A. Bussinger, Bulk parameterization of air-sea exchanges of heat and water vapor including the molecular constraints at the surface, *J. Atmos. Sci.*, *36*, 1722–1735, 1979.

Luther, D. S., A. D. Chave, J. H. Filloux, and P. F. Spain, Evidence for local and non-local barotropic responses to atmospheric forcing during BEMPEX, *Geophys. Res. Lett.*, *17*, 949–952, 1990.

Miller, A. J., On the barotropic planetary oscillations of the Pacific, *J. Mar. Res.*, *47*, 569–594, 1989.

Müller, P., and C. Frankignoul, Direct atmospheric forcing of geostrophic eddies, *J. Phys. Oceanogr.*, *11*, 287–308, 1981.

Niiler, P. P., and C. J. Koblinsky, A local time-dependent Sverdrup balance in the eastern north Pacific Ocean, *Science*, *229*, 754–756, 1985.

Samelson, R. M., Stochastically forced current fluctuations in vertical shear and over topography, *J. Geophys. Res.*, *94*(C6), 8207–8215, 1989.

Samelson, R. M., Evidence for wind-driven current fluctuations in the eastern North Atlantic, *J. Geophys. Res.*, *95*(C7), 11,359–11,368, 1990.

Samelson, R. M., and B. Shrayer, Currents forced by stochastic winds with meridionally varying ampltiude, *J. Geophys. Res.*, *96*(C10), 18,425–18,429, 1991.

Tabata, S., B. Thomas, and D. Ramsden, Annual and interannual variability of steric level along line P in the northeast Pacific Ocean, *J. Phys. Oceanogr.*, *16*, 1378–1398, 1986.

Willebrand, J. S., G. H. Philander, and R. C. Pacanowski, The oceanic response to large-scale atmospheric disturbances, *J. Phys. Oceanogr.*, *10*, 411–429, 1980.

J. Filloux, P. P. Niiler, and J. D. Paduan, Scripps Institute of Oceanography, University of California, La Jolla, CA 92093-0230.

W. T. Liu, Jet Propulsion Laboratory, California Institute of Technology, 4800 Oak Grove Drive, Pasadena, CA 91109-8099.

C. A. Paulson, College of Oceanography, Oregon State University, Corvallis, OR 97331.

R. M. Samelson, Woods Hole Oceanographic Institution, Woods Hole, MA 02543.